Nanoscale

Nanoscale toughening of ultrathin graphene oxide-polymer composites: mechanochemical insights into hydrogen-bonding/van der Waals interactions, polymer chain alignment, and steric parameters

Journal:	*Nanoscale*
Manuscript ID	NR-ART-02-2019-001453.R1
Article Type:	Paper
Date Submitted by the Author:	06-May-2019
Complete List of Authors:	Zhang, Xu; Northwestern University, Department of Mechanical Engineering Nguyen, Hoang; Northwestern University, Department of Mechanical Engineering Daly, Matthew; University of Illinois at Chicago College of Engineering, Department of Civil and Materials Engineering Nguyen, SonBinh; Northwestern University, Dept. of Chemistry Espinosa, Horacio; Northwestern University, Department of Mechanical Engineering

Nanoscale

Nanoscale toughening of ultrathin graphene oxide-polymer composites: mechanochemical insights into hydrogen-bonding/van der Waals interactions, polymer chain alignment, and steric parameters

Received 00th January 20xx,
Accepted 00th January 20xx

DOI: 10.1039/x0xx00000x

Xu Zhang,[^a] Hoang Nguyen,[^a] Matthew Daly,[b#] SonBinh T. Nguyen*[c] and Horacio D. Espinosa*[a,b]

This paper describes a systematic, quantitative study on the nanoscale toughening of monolayer graphene oxide (GO) by an ultra-thin polymer adlayer, which impedes the propagation of cracks during intraplanar fracture. Using molecular dynamics simulations, the crack-bridging capabilities of a library of five hydrogen-bonding-capable polymers are explored against an epoxide-rich GO substrate. The best crack-bridging effect is found in polymers with functional groups that can both donate/accept hydrogen atoms and have better capability to form cooperative hydrogen bonds. Aligning the chains of poly(acrylic acid) orthogonally to the crack propagation direction significantly enhances the fracture toughness of monolayer GO (by 310%) in comparison to that for an adlayer with randomly arranged chains (180% enhancement). Notably, van der Waals interactions, which are seldom highlighted in the fabrication of strong GO-polymers interfaces, are found to also provide significant crack-bridging capabilities when the polymers possess large side groups. These results pave the way for a set of design criteria that can help in remediating the intrinsically brittle mechanical behavior of two-dimensional materials, a barrier that currently restricts their potential applications.

Introduction

Two-dimensional (2D) materials, with exceptional physical properties derived from sub-nanometer thick well-defined atomic structures, hold enormous potential for the development of next-generation devices, including flexible displays and bio-integrated systems such as flexible electronics.[1, 2] However, they tend to exhibit intrinsic brittle fractures,[3, 4] which raises integrity concerns in large-scale applications where defects and stresses are inevitable. Thus, the exploration of toughening strategies for these 2D materials to overcome their intrinsic mechanical weaknesses has emerged as a critical research frontier in recent years.[5] While many chemical insights have been garnered over the past decade,[6] a quantitative understanding of the toughening mechanism is still lacking.

Mechanistically, the strategies that have been proposed for toughening 2D materials can be broadly classified as either intrinsic or extrinsic. Intrinsic toughening includes introducing "traps" ahead of a crack tip to retard crack propagation, either through strain-induced functional groups transformations[7] or by topological defects that can dissipate the crack energies.[8, 9] Extrinsic toughening, on the other hand, requires the deposition of a second material to bridge, and thus impede, a propagating crack through strong interfacial adhesion. Among various 2D materials, graphene oxide (GO) is one in which both types of toughening can be deployed due to its rich and versatile surface chemistry. As a functionalized derivative of graphene, GO possesses a plethora of functional groups including hydroxyl, epoxy, and carboxyl,[10, 11] whose chemical compositions can be tuned at will to afford materials with a broad range of mechanical properties.[7, 12-17] For example, intrinsic toughening in epoxide-rich GO can be enabled through an epoxide-to-ether transition that dissipates energy during tensile loading,[7] resulting in a 100% enhancement in toughness in comparison to a hydroxylated GO. Pathways to extrinsic toughening of GO nanosheets have been demonstrated by the incorporation of polymers that can form an extensive network of hydrogen bonds (HBs) with its surface oxygen functional groups. Indeed, GO has been combined with a variety of hydrogen-bonding-capable synthetic and bio-polymers such as PVA,[18] PMMA,[18] silk fibers,[19] and chitosan,[20] resulting in macroscopic GO-polymer nanocomposites that are stronger and tougher than GO paper alone. While these

[a] Theoretical and Applied Mechanics Program, Northwestern University, 2145 Sheridan Rd., Evanston, IL 60208, USA. E-mail: espinosa@northwestern.edu
[b] Department of Mechanical Engineering, Northwestern University, 2145 Sheridan Rd., Evanston, IL 60208, USA.
[c] Department of Chemistry, Northwestern University, 2145 Sheridan Rd., Evanston, IL 60208, USA. E-mail: stn@northwestern.edu
^These authors contributed equally.
[#] Present address: Department of Civil and Materials Engineering, University of Illinois at Chicago, IL 60607, USA.
Electronic Supplementary Information (ESI) available: [details of any supplementary information available should be included here]. See DOI: 10.1039/x0xx00000x

earlier experiments are highly inspirational, there is a lack of quantitative knowledge on how polymer properties such as chemical compositions and chain conformations may affect the ability of the polymer layer to hinder a propagating crack. Achieving a better understanding of such structure-property relationships would enable the materials engineering community to expand the scope of available GO-based materials beyond the intrinsic toughening of GO itself.

Herein, we report that the fracture toughness of monolayer GO can be increased by 40-180% through the incorporation of an ultra-thin (1.5-4 nm) layer of hydrogen-bonding-capable polymers with the chain randomly distributed on the surface. Up to 310% increase in fracture toughness can be achieved with poly(acrylic acid) if the polymer chains are fully extended and oriented orthogonally against the propagation direction of the crack. This discovery is made possible through a systematic molecular dynamics (MD) study that unravels how the propagation of cracks in a GO nanosheet is impeded by the polymer chains. MD simulations over a small library of hydrogen-bonding-capable polymers enable a comprehensive optimization of the chemical composition, chain conformation, and surface adsorption of the polymer adlayer to allow for the strongest interactions possible with the heterogeneous functional chemistry of the GO sheet, and thus the best fracture toughness. Surprisingly, it reveals that the cohesive bonding between the HB-capable polymer adlayer and the GO surface is also significantly affected by van der Waals (vdW) interactions. Together, these results allow us to establish key design criteria for deploying polymers that can better impede the crack propagation in monolayer GO, suggesting that the range of polymers implemented in GO-polymer nanocomposites can (and should) be extended beyond a selected few that are known to form HBs and π-π-stacking interactions with the GO surface.[6] Such simulation-driven analysis can eventually be generalized to understand toughening in any functionalized 2D material system that does not have HB capabilities.

Results and discussion

Selection of model systems

Recently, Soler-Crespo *et al.*[21] reported that an ultra-thin layer of poly(vinyl alcohol) (PVA) adsorbed on epoxide-rich GO (4:1 epoxide/hydroxyl ratio), fabricated using an experimental Langmuir-Blodgett deposition strategy, can significantly enhance the toughness of GO without sacrificing its native 2D modulus. For GO-PVA nanolaminates, AFM-based indentation tests reveal a three-fold enhancement of load-bearing capability and several-fold increase of energy dissipation in comparison to GO nanosheet. Such enhancements were proposed to arise from a crack-bridging mechanism where the propagation of nanoscale cracks can be obstructed by the stretching of PVA chains over fissures that are as large as 10-20 nm. The strong toughening effect by the polymer chains was made possible due to their multiple-hydrogen-bond interactions with the surface oxygen groups of the GO sheet. These interactions are maximized due to the synergistic matching of the oxidized domain size of the substrate and the length of the adsorbed polymer chain. A similar crack-bridging scheme has also been proposed for a covalently linked graphene-carbon nanotube system,[22] raising the possibility that a general approach for bridging the propagation of cracks can be proposed for a broad range of materials that interact strongly with a 2D nanosheet. Thus, we hypothesize that a systematic tuning of the interactions between the polymer adlayer and the GO sheet can result in an expansion of the scope of available GO-polymer materials through extrinsic toughening. We set out to investigate this idea using an epoxide-rich GO nanosheet model that is similar to that used experimentally by Soler-Crespo *et al.*[21] to favor strong interactions with the hydrogen-bonding-capable polymer adlayer. This in turn will facilitate the comparison of the crack-bridging properties in GO-based nanocomposites by polymers with different chemical and structural features and allow for a clear elucidation of the extrinsic toughening effect from a molecular-level consideration.

For model polymers that can form hydrogen bonds with the epoxide-rich GO, we select five oxygen-containing polymers that have often been used in GO-polymer nanocomposites: poly(acrylic acid),[23] poly(methyl acrylate), poly(vinyl alcohol),[18] poly(butyl acrylate),[24] and poly(ethylene glycol)[25] (abbreviated as PAA, PMA, PVA, PBA, and PEG, respectively). This focused library (Fig. 1) allows for full coverage of the two key factors that affect HB formation between these oxygen-containing polymers and the surface

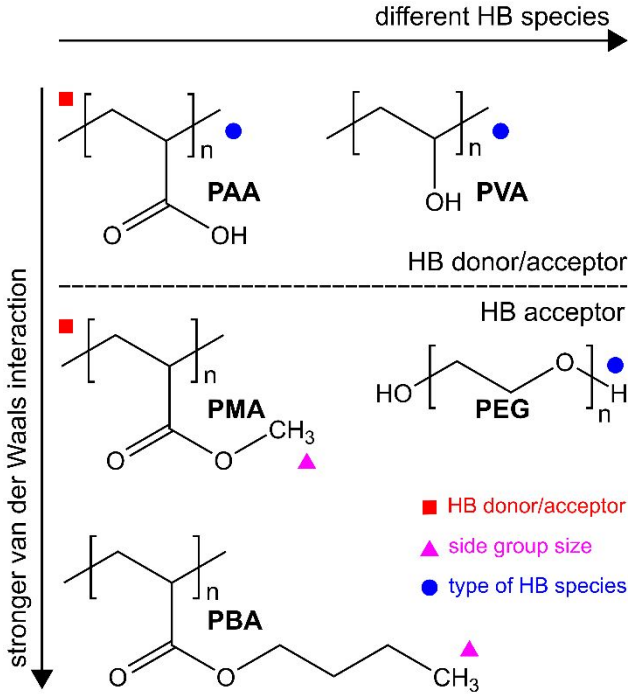

Fig. 1 Model polymer systems including poly(acrylic acid) (PAA), poly(methyl acrylate) (PMA), poly(butyl acrylate) (PBA), poly(vinyl alcohol) (PVA),and poly(ethylene glycol) (PEG) classified according to the type of HB species and relative strength of vdW interactions. Polymer pairs whose performance are compared for specific design criteria, namely, HB donor/acceptor, side group length and type of HB species, are

marked with the same symbols (red square, purple triangle, and blue circles), respectively.

oxygen species of GO: the types of HB species and the "length" of the side group. The three main types of HB species (carboxyl, hydroxyl and ether functional groups) are studied by comparing PAA, PVA, and PEG. Notably, the critical effect of having both HB donor/acceptor in the same polymer are elucidated in the series of two homologous carboxylated polymers (PAA, PMA), with PAA being able to both donate and accept hydrogen atoms (HB donor/acceptor) while PMA only capable of accepting hydrogen atoms (HB acceptor). Comparing PMA to PBA reveals the effect of the side group length. Moreover, the contribution to the toughening from vdW interactions increases for PMA and PBA, which allows us to contrast the toughening effect from HBs with that from vdW interactions.

To be consistent with the GO-PVA experimental system reported by Soler-Crespo *et al.*,[21] we employ a 134-repeating unit (degree of polymerization (DP) = 134) PVA chain and a final polymer thickness of ~ 1.5 nm in our model, equivalent to 6 polymer chains for a 7.5 × 7.1 nm^2 GO sheet and ~ 48 wt % PVA composition. The number of the polymer chains (6) and polymer length (DP = 134) are maintained for the GO-polymer models with the remaining vinyl-typed polymers (PAA, PMA, and PBA), which has 2 C in each repeating unit in the backbone. For PEG, which has 2 C and 1 O in each backbone repeating unit, a polymer chain of equivalent length (DP = 90) is chosen but the number of polymer chain/GO sheet is still maintained at 6.

Adsorption of polymer chains on GO

To explore the toughening effects of polymer adlayers as they would exist in a composite material, we configured our model system as a mixture of GO and polymer melts. Following the approach described in Auhl et al.,[26] we generated polymer chains with melt-state conformations (see Electronic Supporting Information (ESI), Section S1[†]) and maintained their melt-state statistics until they were adsorbed onto the GO surface. After contact, the whole system was kept above the glass-transition temperature of the polymers until the total energy converges to a minimum (see Experimental section). The crack-bridging simulation was then performed after this annealing process. Drawing an analogy from the bridging of cracks in fiber composites, which is controlled by the fiber conformation (embedded length, orientation, etc.),[27] we hypothesize that the extrinsic toughening, or the crack-bridging effect, in our GO-polymer models would be similarly governed by the nanoscale conformation of polymer chains (end-to-end distance and orientation). However, as our vinyl polymer chains are "flexible" on a molecular scale, they can form a multitude of intra- and inter-chains interactions that greatly reduce their end-to-end distance in comparison to their contour lengths (i.e., the length of the polymer at maximum physically possible extension).[28] This in turn will affect the crack-bridging properties of a polymer chain at the nanoscale as its fully extended conformation across a crack is expected to impede the propagation of that crack better than a coiled up one.

Fig. 2a shows the physical probability curves for finding an

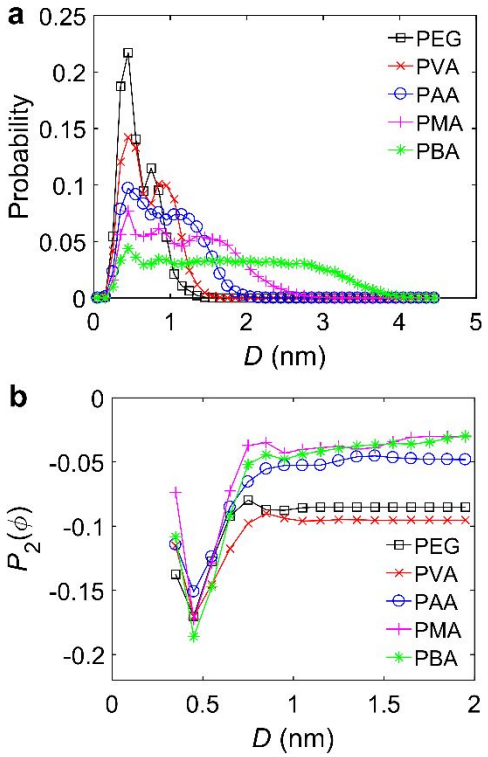

Fig. 2 Adsorption of polymer chains on GO. (a) Probability for polymer atoms at a certain height or distance (D) from the basal plane of GO. (b) The orientational parameter $P_2(\phi)$ of the backbone bond at various distance (D) from the basal plane of GO.

atom from the adsorbed polymer chains at a given height or distance (D) from the basal plane of the GO sheet. These number-density profiles all have a peak at ~0.45 nm, representing atoms that are in direct contact with the GO sheet, or in other words, "closely adsorbed". As the side group of the polymer becomes larger, the proportion of these closely adsorbed atoms decreases, from 0.22 for PEG to 0.04 for PBA. At the same time, the thickness of the polymer adlayer increases, from 1.55 nm for PEG to 4.45 nm for PBA. A second peak at ~1 nm, arising from the non-bonded neighbors of the closely adsorbed atoms, is also visible in the number-density profiles but becomes less obvious with increased side group size, again consistent with the decreased proportion of close-adsorbed atoms. To characterize the extent that the backbone of a polymer chain associates with a surface, we employ the orientation-order parameter $P_2(\phi)$,[29, 30] which is calculated as:

$$P_2(\phi) = \frac{1}{2} < 3\cos^2\phi - 1 > \qquad (1)$$

where ϕ is the angle between the vector that is normal to the surface (i.e., the z-axis, Fig. 3a) and the backbone bonds of the adsorbed polymer chains. Good adsorption occurs when all the backbone bonds are parallel to the adsorbed surface, resulting in $P_2(\phi)$ = −0.5 ($P_2(\phi)$ = 1 when all the backbone bonds are perpendicular to the surface, and $P_2(\phi)$ = 0 when

the backbone bonds adopt random orientations). Fig. 2b shows the plots of $P_2(\phi)$ for the five polymers in this study at various distances D from the GO surface. Consistent with the

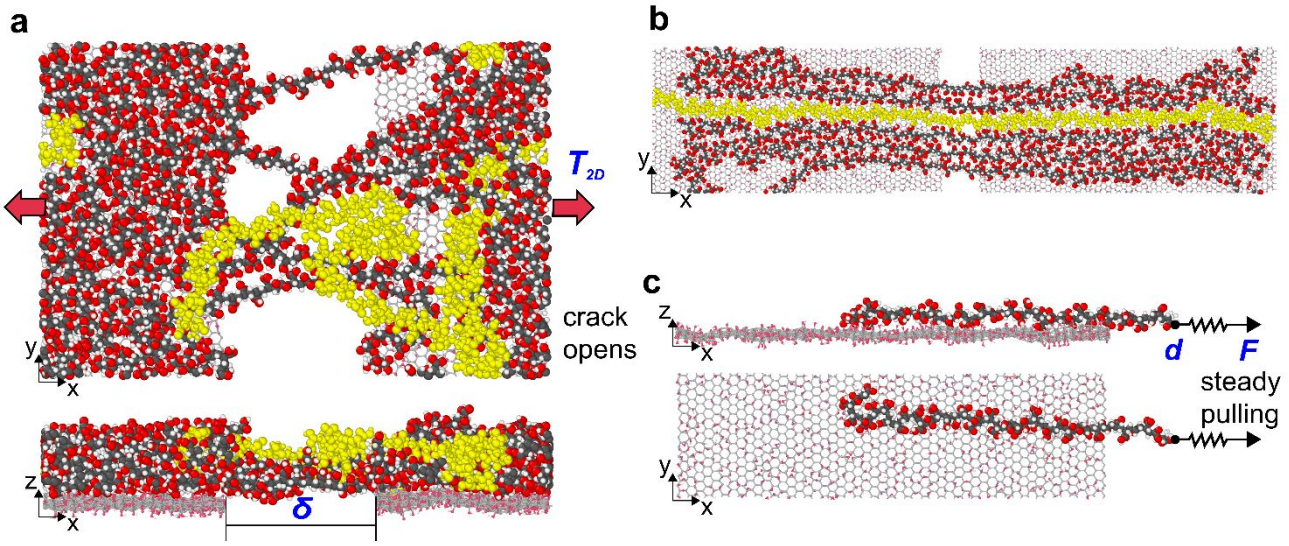

Fig. 3 Schematic illustrations of the GO-PAA simulation system in this study. Carbon atoms are colored grey, oxygen atoms are colored red, and hydrogen atoms are colored white. To contrast with the polymer, the GO molecules have been reduced in their relative sizes. When the simulation comprises multiple polymer chains, as in panels (a) and (b), one representative polymer chain is highlighted in yellow to make visualization easier for the readers. (a) A crack-opening simulation where polymer chains are randomly adsorbed on a pre-cracked GO prior to its opening. Our model comprises six 134-repeating unit polymer chains adsorbed on a 7.5 × 7.1 nm^2 GO sheet and a final polymer thickness of ~ 1.5 nm (~ 60 wt % PAA). The number of the polymer chain (6) and polymer length (DP = 134) were maintained for all the four GO-vinyl-functionalized polymer models (PAA, PMA, PBA, and PVA), which have 2 C in each repeating unit in the backbone. For PEG, which has 2 C and 1 O in each backbone repeating unit, the equivalent polymer was chosen as a chain with DP = 90 but the number of polymer chain/GO sheet was still maintained at 6. The 2D traction (T_{2D}) was recorded as a function of the crack-opening (δ). (b) An ideal crack-opening scenario with all six polymer chains close to their contour length and aligned orthogonally to the crack-propagation direction. (c) A single-chain pull-off simulation where a single polymer chain (DP = 40 for vinyl polymer models, and DP = 27 for PEG) is pulled off from the surface of GO with a spring force at a constant velocity. The pulling force (F) and the displacement (d) of the carbon atom being pulled along the x-direction were measured.

ultrathin nature of the polymer adlayer, the $P_2(\phi)$ plots for all five GO-polymer models exhibits a minimum negative value at ~0.45 nm, the distance of the closely adsorbed backbone atoms.

Crack-opening simulations

To quantify the toughening effect of the various polymers investigated herein, we implement Rice's J-integral approach,[31] which captures non-linear crack-tip-toughening processes that occur in materials that do not behave in an elastic fashion, as have been observed for GO nanosheets.[7, 17] As well-known in the literature for fiber-reinforced composites,[27, 32, 33] the presence of a small amount of reinforcing fibers in a material can greatly enhance its ability to resist the propagation of developing cracks. The presence of fiber effectively allows for the development of a process zone (i.e., the region of space surrounding the crack tip) whose size is not negligible compared to the crack length, thus invalidating the fundamental assumption of linear-elastic fracture mechanics. In the case of macroscopic fiber-reinforced composites, good bridging fibers can effectively resist the further opening of a large crack by dissipating a significant amount of energy through the decohesion of the fiber-matrix interface beyond the intrinsic fracture energy of the matrix itself.[32] We thus envision that a similar mechanism will arise in the GO-polymer systems examined in this work where the polymer chains can bridge a developing nanoscale crack by anchoring to the GO sheet through HBs.

Unlike many brittle materials whose fracture energy can be characterized solely by a single number G_0, the critical energy release rate, the resistance of polymer-toughened GO composites must be described by a resistance (R) curve (see ESI, Fig. S1[†]), whose steady-state value can be estimated by calculating the 2D energy release per unit distance following the established J-integral approach for a fiber-reinforced system:[27, 32, 33]

$$G_c = J_c = G_0 + G_f = G_0 + \int_0^{\delta_c} T(\delta)d\delta \qquad (2)$$

where G_c is the critical energy release rate (expressed in energy/distance unit) of the composite, G_f is the energy release rate due to bridging, T is the traction between the crack surface, and δ_c is the size of the critical crack-opening after which T vanishes. As described in the ESI, Section S2,[†] G_c is calculated by super-imposing G_0 (the critical energy release rate of GO, found to be 4 nJ/m for GO monolayers as the average of a hydroxyl-rich GO (3.4 nJ/m) and an epoxide-rich GO (4.6 nJ/m)[15, 34]) and the energy dissipation from the polymer G_f. As the value of G_0 implicitly "contains" information for an already initiated and propagated crack,[33] we can investigate the non-linear effects of polymer toughening in GO by examining only the process of crack-opening (i.e., behind the crack tip).

We note in passing that while eq 2 is derived for a continuum system with homogeneous distribution of masses, and we used atomistically discrete molecular models in our MD simulation, the physics that underline Rice's J-integral formalism still hold. The molecular models are simply used as representative volume elements (RVEs) to estimate the behavior of the material in the energy-dominated regime, where the crack size is much larger than their dimensions. At such a scale difference, local mass fluctuations caused by non-uniform distributions of polymer chains are negligible and the entire system is considered "homogenized".

Fig. 3a shows the schematic of our crack-opening simulation, which involves multiple polymer chains that were randomly adsorbed on a pre-cracked GO sheet (see ESI, Video 1† for a movie of the polymer chain motions). We calculated the crack-bridging force provided by the polymer and then divided the force by the width of GO (the y dimension in Fig. 3a) to obtain the 2D traction (T_{2D}) as a function of the crack opening (δ) (see Fig. 4a and ESI, Section S3†). As expected, T_{2D} decreases as the crack-bridging chains are being pulled off from the GO surface and their stick-slip motions can be observed as irregular "peak-valley" patterns along the diminishing traction profile. To quantify the crack-bridging effect, we calculated the 2D energy release rate G_f (Fig. 4b, see also ESI, Table S2† for the full datasets) for all polymers by integrating the areas under the T_{2D} profiles (Fig. 4a and ESI, Section S3†). From this data, the enhancement in GO-fracture toughness due to the polymer crack-bridging effect ($(G_c\text{-}G_0)/G_0$ which is G_f/G_0), is 40-180% (Fig. 4c), comparable to that observed experimentally (up to 200%) for an ultrathin GO-PVA nanocomposite.[21]

As shown in Fig. 4b, the crack-bridging performances of the four vinyl-functionalized polymers (PAA, PMA, PVA and PBA) randomly adsorbed on GO, as represented by the blue bars, are better than that for PEG, albeit with large standard deviations that can partially be attributed to the discrepancy between the large number of possible starting conformations by the six polymer chains in this system (an ideal conformation will be described in the next paragraph) and the limited number of possible replica simulations. Nevertheless, assuming that G_f follows a Gaussian distribution, we used the Student's t-distribution to compare the G_f values between pairs of polymers to elucidate the toughening effect by the different types of HB species and the length of the side group. At 95% level of confidence, such analysis reveals that the G_f of PAA is larger than those of PMA (p-value[35] = 0.042) and PVA (p-value = 0.048). However, the suggestion that the G_f of PAA is larger than that of PBA, which in turn is larger than the G_f of PMA, can only be made at ~80% level of confidence.

To better quantify the crack-bridging effect of each of the five polymers in this study, we reduced the large number of possible starting conformations for the nanocomposite down to an ideal crack-bridging scenario where all of the polymer chains were adsorbed onto the GO surface at their contour length and were aligned orthogonal to the crack propagation direction, as shown in Fig. 3b. These systems were then equilibrated following the same procedure used for the random conformation case. We further constrained the simulation to have all chains being simultaneously pulled off from the same side of the crack. The obtained G_f values for the five models in this idealized scenario, represented as green bars in Fig. 4b, are consistently much higher than those for the randomly adsorbed case (blue bars in Fig. 4b). Notably, the G_f value for the PAA provided the best crack-bridging effect, with 310% enhancement (Fig. 4c) in fracture toughness! While not directly comparable, this value is very similar to that recently modeled for the covalently linked graphene-CNT system[22](360% enhancement in energy release rate with completely aligned CNT arrays), suggesting that excellent extrinsic toughening in GO-based nanocomposites can indeed be achieved with ultrathin soft polymer adlayers as long as strong chemical interactions can be engineered into the system. Notably, the optimal G_f values for these ideal crack-bridging simulations have a strong positive correlation with the average G_f of the aforementioned randomly adsorbed GO-polymer models (correlation coefficient of 0.9848), allowing us to increase the level of confidence in the latter set of data, and conclude that PAA > PBA > PVA > PMA > PEG in crack-bridging. As experiments that can verify such a relationship would require an enormous amount of effort in both fabrication and measurement of the types recently reported,[21] our MD predictions can serve as a facile pre-screen prior to the more expensive and time-consuming experimental phase.

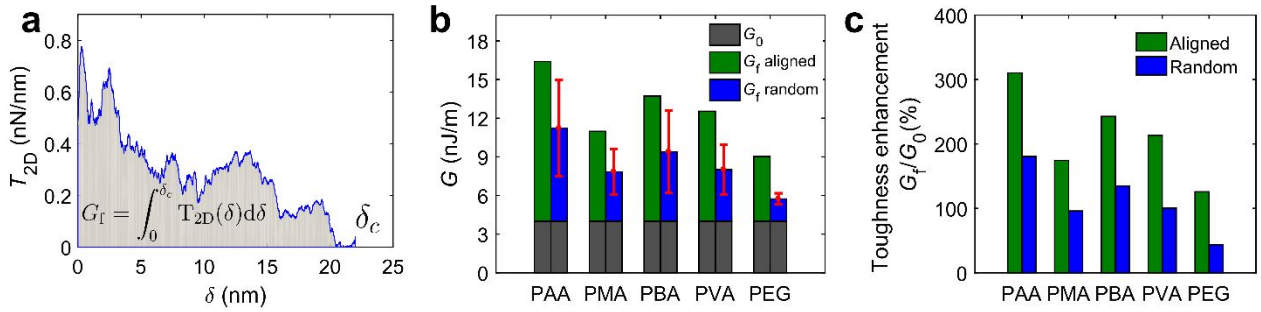

Fig. 4 Results of the crack-opening simulations. (a)A typical 2D traction (T_{2D}) – crack opening (δ) curve of a GO-PAA system. (b) 2D energy release rate G for the GO and GO-polymer systems. G_0 represents the 2D energy release rate of GO itself. G_f values were calculated by numerically integrating the $T_{2D} - \delta$ curve for all polymers. The blue bars are G_f values of the polymers with random chain arrangements (Fig. 3a). The sample standard deviations were calculated from six simulations, a small number that limited by our available computational resources (ESI, Section S6†). The green bars correspond to cases where all polymer chains are aligned orthogonal to the crack propagation direction and

contribute to the crack-bridging (Fig. 3b). (c) Enhancement of the fracture toughness of GO from the adsorbed polymers with aligned and random chain conformations. The enhancement was calculated as G_f/G_0. The average G_f values were used for the random cases.

In addition to the fracture energy, nanoscale fracture behavior has also been proposed to be governed by a "characteristic size" of the flaw-tolerance phenomena,[32, 36] which can potentially be modified by the polymer adlayer. In our estimation, the presence of the polymer adlayer should have a minimal effect on the intrinsic characteristic size of the GO sheet. When the defect size is smaller than the characteristic size, where the strength of the material controls the failure, the absorbed un-stretched polymer chains, which have a much lower stiffness than GO; would have a negligible contribution to relieving the stress concentration in GO and thus does not affect its characteristic size. On the other hand, for defects that are larger than the characteristic size, in the energy-dominated regime, the adlayer can provide an extrinsic toughening to GO, as shown herein. In essence, while the polymer adlayer does not prevent fracture initiation from defects, it does contribute to resisting its growth.

Single-chain pull-off simulations

To understand the aforementioned trend in crack-bridging simulations in terms of HB donor/acceptor effect, the length of the side groups, and the type of HB species, we carried out single-chain pull-off simulations (Fig. 3c) for each of the adsorbed polymer model, starting from the ideal crack-bridging configuration of the polymer chain being orthogonal to the propagation direction the crack. To reduce the computational cost and increase the statistical accuracy, we decreased the system size (the polymer length was shortened to ~ 1/3 and the GO area was reduced by ~1/2) and assumed a configuration where each of the polymer chain initially resided on one side of the crack. The polymer was then pulled off from this one side, essentially constraining the polymer motion to only "one GO surface". In this configuration, all polymer chains started with similar contour length and followed similar motion paths, so the difference in their cohesive behaviours can be solely attributed to the chemical properties of the polymer. Following an approach that was applied to simulate the motion of hydrogen-bonding-capable polypeptides on hydroxylated substrates,[37] the polymer chain was pulled off the GO surface with a spring force (F) at a constant velocity (Fig. 3c). During the pull-off simulations, we measured F as a function of the displacement (d) of the polymer carbon atom to which the spring was connected. Since we pulled the chain off at a constant velocity, the spring force varied as a function of the instantaneous GO-polymer interactions, allowing for the "detection" of stick-slip motions that were proportional to the magnitude of the interaction energy with the GO surface.

As shown in Fig. 5a, the *F-d* curve for the GO-PAA system clearly displays a jagged sawtooth pattern that is indicative of the expected stick-slip behaviour for a PAA chain that forms multiple HBs with the GO surface (see ESI, Video 2,† for the movie of this simulation). As the pulling initiates, multiple HBs serve as anchoring points to the GO surface, causing the PAA chain backbone to stretch and giving rise to local increases of the pulling force (stick stages). Rupturing these HBs releases the stored elastic energy and leads to a sudden drop in the pulling force (slip stage), where interfacial sliding occurs. After this slip, HBs quickly reform between the GO surface and the next repeating unit of the PAA chain, building up to the next rupture/slip event and ultimately resulting in several stick-slip transitions throughout the polymer pull-off process. As the values for F and d of the stick-slip events are larger than those for the rupture of a single hydrogen bond, each slip event must involve the rupture of HBs in a cluster fashion.[38] The average number of HBs that rupture in such a cluster can then be estimated from the release of elastic energy,[38] as shown below (see *Evaluation of chemical effects in single chain pull-off simulations* section).

Fig. 5a shows a gradual decrease in the pulling force as the polymer chain in our PAA-GO model is pulled off the GO surface, not surprisingly, due to the decrease in polymer-GO interactions. Normalizing this force by the number of repeating units (N) that are instantaneously adsorbed on the surface of GO shows that the per-repeating-unit force (F/N) remains at a steady-state value of 0.045 ± 0.004 nN (red line in Fig. 5b; see ESI, Section S4† for the other *F-d* profiles) up to a displacement of 5 nm (~ ½ of the initial polymer length), suggesting that it can be used to represent the average force that each repeating unit of the polymer chain "exerts" on the GO surface when the opening of the crack is ≤ ½ the length of the polymer chain. As such, this average F/N value can be correlated to the strength of interactions between each repeating unit of the PAA chain with the GO surface, and thus its overall crack-bridging behaviour.

Indeed, the trend in F/N data (Fig. 5c) for all of our polymers tracks quite well with the trend in the molar per-repeating-unit binding energy E/N, suggesting that the pulling force exerted on the GO surface by each type of polymer can be understood in terms of the chemical interactions as parameterized by the MD force fields.[39] Additionally, as E/N can be decomposed into Lennard-Jones (LJ) and Coulombic (Coul) energies, the strength of the interactions between each polymer chain and the GO surface can be further quantified in terms of vdW and HB interactions,[40] respectively (Fig. 5d).

Comparison between the multi-chain crack-opening and single-chain pull-off simulations

While the single-chain pull-off simulations can be considered simplified snapshots of our multi-chain crack-opening simulations, the PBA ≥ PAA > PMA > PVA > PEG trend in F/N data (Fig. 5c) does not quantitatively agree with the PAA > PBA > PVA > PMA > PEG trend in G_f data (Fig. 4b). Together with the larger-than-Coulombic LJ contributions to E/N data found for PBA and PMA (Fig. 5d), this discrepancy highlights the significant capability of vdW interactions to provide good crack-toughening interfaces. Taken one step further, this observation suggests that the scope of polymer adlayers that can toughen GO-polymer nanocomposites can (and should) be

extended to include polymers that have good vdW interactions with the GO surface in addition to the few that were historically chosen due to their perceived abilities to form strong HBs and π-π-stacking interactions with GO.[6] While the of potential GO-polymer composites. For example, our work

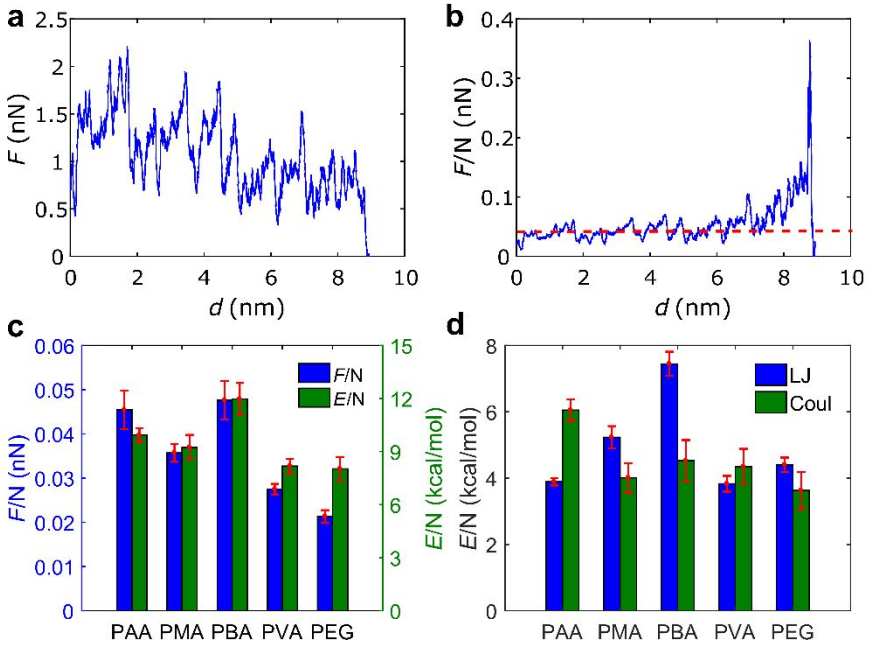

Fig. 5 Results of the single-chain pull-off simulations for models comprising a 9.7-nm-long polymer chain (27 repeating units for PEG and 40 for all other polymers) adsorbed on an 11 × 3.2 nm² GO sheet. (a) A representative pulling force (*F*) vs displacement (*d*) curve for the GO-PAA system. (b) The force in Fig. 5a normalized by the number of repeating units (N) that were instantaneously adsorbed on the GO surface. The red dashed line corresponds to the average of the *F*/N data from 0-5 nm. For (a)-(b), the data shown were processed through a forward-moving average filter over 20 points. (c) The average per-repeating-unit force (*F*/N) and molar binding energy (*E*/N) for all five polymer models. The average *F*/N value is defined as the average of the *F*/N data for each polymer in the 0-5 nm displacement range. The average *E*/N is defined as the molar per-repeating-unit change in the GO-polymer interfacial energies between the ½-pull-off stage (i.e., ~ ½ of the initial polymer chain has been pulled off) and the minimum-energy state before any of the repeating unit is pulled-off. (d) *E*/N for all five polymer models, separated into Lennard-Jones (LJ) and Coulombic (Coul) energies. For (c) and (d), the error bars represent sample standard deviations that were calculated over five replicates of simulations.

herein clearly shows that replacing the carboxyl groups in PAA with the carboxymethyl group in PMA can increase the LJ contribution to *E*/N to exceed the Coul component (Fig. 5d). Further increase of the size of the ester group to a larger carboxybutyl group, as in PBA, increases the LJ contribution to *E*/N to almost twice that of the Coul component, and this leads to the *F*/N value for PBA being comparable to PAA in the single-chain pull-off simulation. Supporting this notion is the recent report that polydimethylsiloxane (PDMS), which primarily interacts with GO through vdW interactions, significantly enhances the toughness and stiffness of graphene-based nanocomposites in comparison to GO foam (28× higher toughness and 65× higher stiffness with 1.5 wt % of PDMS).[41, 42]

Interestingly, while the G_f value of PVA is almost twice that of PEG in the multi-chain crack-opening simulation (Fig. 4b), its *F*/N value is quite similar to that of PEG in the single-chain pull-off simulation (Fig. 5c). Given the identical atomic composition between these two polymers (repeating units = C_2H_4O) and the better "packing" of the PEG chains on the GO surface (Fig. 2a), this inconsistency can only be attributed to the additional crack-bridging effect from a network of hydrogen-bonded polymer chains produced by inter-chain HBs in the GO-PVA case, as has been proposed to explain experimental crack-toughening.[6, 43] This is akin to the case of fiber-reinforcement concrete where a network of "crack-bridging" struts can lead to vast improvements in the ability of the matrix to impede the crack propagation.

That PBA and PAA both have similar *F*/N values in the single-chain pull-off simulations (Fig. 5c) but large differences in G_f data in the multi-chain crack-opening simulations (Fig. 4b) further indicates a clear reduction in the ability of a randomly distributed multi-chain PBA film to bridge a developing crack in comparison to PAA. This is presumably due to a reduction of GO-polymer interactions: the large carboxybutyl side groups of the PBA chains do not allow them to pack in the adlayer in a manner that maintains the most optimal interactions between each polymer chain and the GO surface, as confirmed by the lower proportion of closely absorbed atoms for PBA when multiple chains are present (Fig. 2a). In such a situation, polymer-polymer inter-chain vdW interactions presumably increase at the expense of GO-polymer interactions. In the next section, we will make an attempt to quantify the relationship between chemical effects, such as the types of hydrogen bonds and their number, and the crack-toughening mechanism.

Evaluation of chemical effects in single chain pull-off simulations

The per-repeating-unit strength of the HB interaction that our five polymers make to the GO surface can also be obtained from the single-chain pull-off simulations as the dimensionless quantity N_{HB}/N (Fig. 6a; see Experimental Section and ESI, Section S5[†] for N_{HB}/N datasets). This value allows us to separate our five models into two classes: those that can only accept hydrogen atoms (PMA, PBA, and PEG) and those that can both accept and donate hydrogen atoms (PAA and PVA).

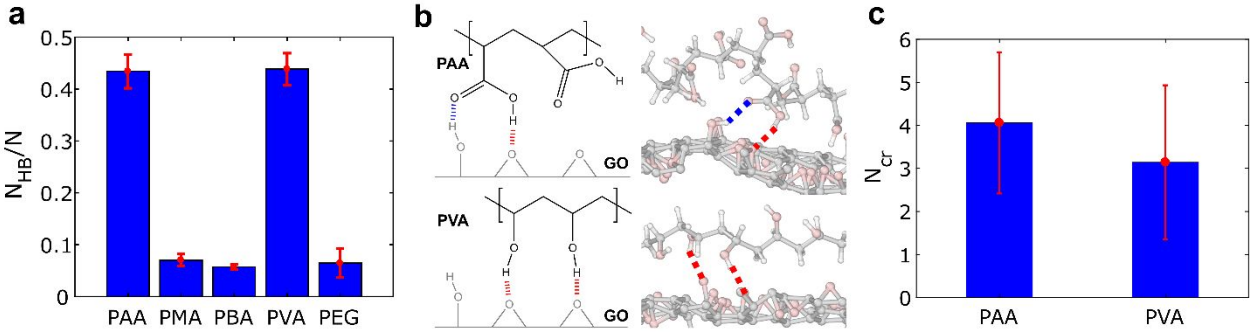

Fig. 6 HB analysis in the single-chain pull-off simulations (a) The number of HBs observed between the polymer chain and GO normalized by N (N_{HB}/N) for all five polymer models. HBs were count with a criterion of donor-acceptor distance < 3.5 Å and H-acceptor-donor angle < 30°,[44] and were count up to 5 nm displacement. The error bars represent sample standard deviations that were calculated over five replicates of simulations. (b) Illustration (left) and simulation snapshots (right) of cooperative HBs formed at the interface in the PAA and PVA system. For PAA, a cooperative HB pair can form within one repeating unit, where the carbonyl oxygen and hydroxyl group each forms a hydrogen bond, as shown by the blue and red dashed lines, respectively. For PVA, two repeating units are required to form a cooperative HB pair, where one hydrogen bond forms in each repeating unit. In the snapshots, carbon atoms are colored grey, oxygen atoms are colored pink, and hydrogen atoms are colored white. (c) Number of hydrogen bonds (N_{cr}) that are cleaved in a single stick-slip motion for PAA and PVA.

Notably, comparing PAA and PMA, whose carboxyl side groups are roughly of the same size, offers clear insights into how these different HB capabilities are translated into very different Coul contributions. With its carboxyl groups capable of both donating and accepting HBs, PAA can form more HBs with our epoxide-rich GO surface (epoxide groups are HB acceptors) in comparison to PMA (Fig. 6a), resulting in a higher Coul contribution (Fig. 5d, cf Coul energies). Although the methoxy groups of PMA do provide some vdW interactions, the accompanying energy gain (Fig. 5d, cf LJ energies) does not adequately compensate for the loss of HB interactions, thus yielding lower overall *E*/N and *F*/N data (Fig. 5c). Such a comparison clearly indicates the advantage that polymers with both HB donors and acceptors have over those with only HB acceptors in providing stronger interface with the GO sheet and thus better mechanical performance for the corresponding GO-polymer composite. This conclusion is consistent with that reported in a previous experimental study,[18] where GO-PVA nanocomposites show better mechanical properties than GO-poly(methyl methacrylate) nanocomposites because the latter polymer adlayer is only capable of accepting hydrogen atoms.

Interestingly, while PVA shows an N_{HB}/N value that is 570% higher than that for PEG, this difference only manifests in ~ 29% increase in *F*/N. In contrast, PAA, which has the same N_{HB}/N value as PVA but with one more "CO" in its side group, shows almost 100% increase in *F*/N value than PEG. This difference can be explained by the better ability of PAA to form a cooperative HB pair with the epoxide-rich GO surface using just one repeating unit in the polymer chain (Fig. 6b). This is in contrast to PVA, which requires two adjacent repeating units to form such a pair (Fig. 6b). In other words, a single carboxyl group in a PAA repeating unit can form a cooperative HB pair (or participate in larger cooperative HB clusters) that would be broken in concerts in a pull-off experiment,[38] resulting in a stick-slip motion that has larger *F* and *d* values than those for the rupture of a single hydrogen bond. A similar stick-slip event in the GO-PVA model would require two hydroxyl groups from adjacent repeating units, leading to fewer possibilities for stick-slip transitions. Indeed, a rupture strength analysis[38] (see Experimental Section) reveals that one stick-slip motion in PAA requires the cleavage of ~4 hydrogen bonds (vs 3 for PVA; see Fig. 6c and ESI, Section S5[†]), resulting in a higher friction force observed for PAA. This finding is also consistent with the report that incorporating carboxyl-functionalized multi-walled carbon nanotubes (MWCNT) into polymer-MWCNT composites can lead to better mechanical properties than hydroxyl-functionalized MWCNT.[45]

Conclusions

In summary, we have shown that the presence of an ultra-thin adlayer of oxygen-containing hydrogen-bonding-capable polymers on a monolayer epoxide-rich GO can greatly enhance the fracture toughness of this monolayer. With random chain arrangements, the largest enhancement (180%) is found for PAA, whose carboxylate side groups intrinsically place an HB-acceptor and HB-donor moiety close in space, facilitating the formation of cooperative HB clusters that synergistically enhance the interaction of the polymer with the GO surface. The breaking of cooperative HB clusters manifests into stick-slip motions of polymer chains with friction-force magnitudes that are several times larger than the breakage of a single HB. The enhancement further improves to 310% when the PAA

chains are orthogonally aligned to the crack propagation direction of GO. For PMA and PBA whose carboxylate ester groups are only HB acceptors, the enhancements are slightly inferior to that of PAA but are still in an impressive 175-243% range with orthogonally aligned polymer chains. Our MD analysis clearly captures an increase in the overall LJ contribution from these polymers as a function of the length of their side groups. While this vdW contribution can potentially be restricted by the limited packing efficiency, which manifests as larger polymer thicknesses in PMA and PBA, it contributes significantly to the crack-bridging properties, resulting in non-negligible fracture toughness enhancements. Notably, a fully aligned polyethylene (PE, DP = 134) adlayer with the same steric properties as PEG but without the ability for HB formations, can result in an 83% enhancement of GO fracture toughness (ESI, Table S2†), highlighting the importance of vdW interactions.[46]

Our data strongly advocate three design criteria for rendering ultrathin GO-polymer nanocomposites that are resistant toward nanoscale cracks: 1) Maximizing the formation of cooperative HB clusters between the polymer adlayer and the GO surface; 2) Aligning the polymer chains orthogonally to the crack propagation direction; and 3) Increasing the vdW interactions for polymers that do not have both HB-donors and -acceptors. For GO, these criteria suggest that the range of polymers implemented for GO-polymer nanocomposites should be extended beyond a selected few that are known to form HBs and π-π-stacking interactions with the GO surface.[6] Most importantly, the last criterion opens up the possibility for toughening a broad range of 2D materials that do not have HB-forming capabilities.

We note in passing that while GO has reduced modulus and strength with respect to graphene[7] due to the presence of functional groups on its basal plane, these groups can actually render GO more damage-tolerant through an intrinsic toughening mechanism.[7] In addition, they provide possibilities for extrinsic toughening of the GO sheet through interactions with polymer adlayers as shown in this work. By applying a bottom-up materials-by-design strategy, one should be able to optimize the functional-group compositions of GO as well as their spatial distributions to maximize desirable mechanical properties for a particular GO-polymer system. Such investigation can provide important insights into the design of next-generation strong and tough composites.

Lastly, we note that as our current study was primarily aimed to unravel the chemical basis for nanoscale toughening by a polymer adlayer, we did not consider process-related conditions (degree of thermoset cure, polymer chain mobility and crystallinity etc.) and/or mixed-mode phenomenon (e.g., the deflection of the crack propagation due to the adsorbed polymers). While these have been known to affect the fracture toughness, their complexity necessitates the consideration of larger model systems and more specific force fields and would render the computation prohibitively expensive.[22]

Experimental section

General considerations

The simulations were performed on the Stampede2 cluster at the Texas Advanced Computing Center (TACC), University of Texas at Austin, and the Quest cluster at Northwestern University. The CHARMM general force field (CGenFF)[47] was used to model the GO-polymer system. The atomic charges and force field parameters for bonded interactions of polymer molecules were obtained from the CGenFF program (interface version 1.0.0, force field version 3.0.1)[48] by uploading *training structures* of each polymer with 10 repeating units. The Lennard-Jones parameters for polymers were obtained from CGenFF C36 version.[47, 49] The force field parameters for GO were taken from Fonseca et al.[50] GO flakes were generated by a Monte Carlo Algorithm described in an earlier work[17] with seventy percent of the carbon atoms oxidized and a 4-to-1 epoxide-to-hydroxyl group ratio. Polymer chains were generated by a self-avoiding random walk method. The Large-scale Atomic/Molecular Massively Parallel Simulator (LAMMPS) software package[51] was used to run MD simulations. The timestep was set to be 1 fs, and the inner and outer cutoff distances for non-bonded interactions were set to be 10 and 12 Angstroms, respectively.

Crack-opening simulations

For these simulations, a pre-cracked GO flake with dimensions measuring 7.5 × 7.1 nm was created by cleaving the GO plane along the armchair or zigzag direction of GO and separating the cleaved surfaces by 2 Å. Six atactic polymer chains with their average mean-square end-to-end distance corresponding to their melt states (detailed in ESI, Section S1†) were suspended over the GO flake. The contour length was kept to be 32.5 nm for all polymers (90 repeating units for PEG and 134 repeating units for all the other polymers). The GO flake is large enough to adsorb a polymer chain without affecting its end-to-end distance. Periodic boundary conditions were applied in all directions with a ~9 nm vacuum above and below the GO-polymer system in the z-direction. To facilitate the polymer adsorption, the polymer chains were pushed against the GO with a potential wall at 650K for 0.1 ns, during which the polymer chains interacted via a soft repulsive potential to maintain their melt-state statistics. Upon contact with the surface, the potential wall was removed, and the normal potential was re-established. This process simulated an idealized melt-spinning of polymer on GO where the polymer chains were not affected by solvation and the polymer contour length was maximized against phase separation or intramolecular interactions.

After energy minimization using the steepest descent algorithm, the system was kept at 650 K under an *NVT* ensemble for 4 to 8 ns (the time to achieve energy convergence varies between polymers) and then annealed to 300 K for 1 ns. During the equilibration, the motion of GO atoms was restricted with a soft spring in all directions to avoid rigid body motion. After equilibration, the simulation box was deformed in the direction perpendicular (in-plane) to

the crack with a strain rate of 10^9/s. We note that while this strain rate is unrealistic in comparison to what can be achieved in experiments, it can ensure convergence as shown by a previously reported sensitivity analysis[21] as well as in this work (see ESI, Section S3†). Only the coordinates of GO atoms were mapped into the new box to avoid artificial stretching of the polymer phase. The stress (with a unit of stress × volume) in the polymer phase was calculated by summing the per-atom virial stresses of all polymer atoms. Then, it was divided by the x dimension of the box (see Fig. 3a) to calculate the crack-bridging force and then divided by the y dimension of the box to calculate 2D Traction (T_{2D}, with a unit of force/length). A moving average filter of 20 steps was applied to smooth T_{2D}. A total of six simulations (three with the pre-crack along the armchair direction and three along the zigzag direction) were performed for each polymer, in which the location of the crack was changed while keeping the same initial polymer configuration, thus providing different polymer configurations over the crack.

Single-chain pull-off simulations

For these simulations, one chain at its contour length was adsorbed onto an 11 × 3.2 nm^2 GO flake. The contour length was kept to be 9.7 nm for all polymers (27 repeating units for PEG and 40 for all other polymers). Periodic boundary conditions were applied in the y-direction (see Fig. 3c). The system was equilibrated in an *NVT* ensemble at 300K for 1 ns, during which the out-of-plane undulation of GO was restricted by applying spring supports in the y- and z- axes. The steered molecular dynamics (SMD) method was used to pull the backbone carbon atom at the terminal group with a spring with a spring constant of 100 kcal/mol·Angstrom at a constant velocity of 3.8 m/s, during which the pulling force (*F*) and the displacement of the carbon atom (*d*) were measured. The pulling velocity was consistent with the strain rate used in the crack opening simulations, and was slow enough for the HBs to reform after a stick-slip event. Throughout the simulation, the rigid body motion of GO was restricted by applying spring supports. A total of five simulations were performed for each polymer in which different initial velocities for atoms were generated. The HBs between the polymer and GO were counted with a criterion of donor-acceptor distance < 3.5 Å and H-acceptor-donor angle < 30°.[44] The N_{HB}/N values were calculated by dividing the total number of simulation-observable HBs that the polymer chain made with the GO surface by the number of monomers on the surface of GO (N) at the corresponding timestep. To compare the crack-bridging effects in HB-dominated PAA- and PVA-GO models, we adopted a methodology that was used to study the collective effect of HBs on rupture strength in HB assemblies.[38] We simulated two deformation modes of polymers on GO: out-of-plane peeling and in-plane shear (same as the single-chain pull-off) (ESI, Fig. S4†). In the peeling mode, HBs were cleaved sequentially (i.e., one by one) from the GO surface; however, multiple HBs can be cleaved simultaneously in the shear mode in one stick-slip motion. We found the average rupture force of one cleavage (peeling mode) and one stick-slip motion (shear mode) (see ESI, Section S5†), and calculated the ratio of the average force in the shear and peeling mode (N_{cr}), which revealed how many HBs were cleaved simultaneously in one stick-slip motion. Visualization and post-analysis of the system were accomplished with OVITO.[52]

Conflicts of interest

The authors claim no conflict of interests.

Acknowledgements

H.D.E. gratefully acknowledges support from NSF through awards No. DMR-1408901 and DMREF-CMMI-1235480, ARO through awards No. W911NF1510068. H.D.E. and S.T.N additionally acknowledge support from the ARO through MURI Award No. W911NF-08-1-054. The authors acknowledge the computational resource provided by the Extreme Science and Engineering Discovery Environment (XSEDE) under proposal TG-MSS140028, as well as the Quest High Performance Computing Cluster at Northwestern University. The authors thank Prof. Jeffrey T. Paci for the helpful discussions. M. D. would like to acknowledge financial support under the Postdoctoral Fellowships Program (Application No.: PDF-502224-2017) from the Natural Sciences and Engineering Research Council (NSERC) of Canada.

Notes and references

1. Y. D. Kim, H. Kim, Y. Cho, J. H. Ryoo, C. H. Park, P. Kim, Y. S. Kim, S. Lee, Y. L. Li, S. N. Park, Y. S. Yoo, D. Yoon, V. E. Dorgan, E. Pop, T. F. Heinz, J. Hone, S. H. Chun, H. Cheong, S. W. Lee, M. H. Bae and Y. D. Park, *Nat. Nanotechnol.*, 2015, **10**, 676-681.
2. B. Radisavljevic, A. Radenovic, J. Brivio, V. Giacometti and A. Kis, *Nat. Nanotechnol.*, 2011, **6**, 147-150.
3. Y. C. Yang, X. Li, M. R. Wen, E. Hacopian, W. B. Chen, Y. J. Gong, J. Zhang, B. Li, W. Zhou, P. M. Ajayan, Q. Chen, T. Zhu and J. Lou, *Adv. Mater.*, 2017, **29**.
4. P. Zhang, L. L. Ma, F. F. Fan, Z. Zeng, C. Peng, P. E. Loya, Z. Liu, Y. J. Gong, J. N. Zhang, X. X. Zhang, P. M. Ajayan, T. Zhu and J. Lou, *Nat. Commun.*, 2014, **5**.
5. D. Akinwande, C. J. Brennan, J. S. Bunch, P. Egberts, J. R. Felts, H. Gao, R. Huang, J.-S. Kim, T. Li and Y. Li, *Extreme Mechanics Letters*, 2017, **13**, 42-77.
6. S. J. Wan, J. S. Peng, L. Jiang and Q. F. Cheng, *Adv. Mater.*, 2016, **28**, 7862-7898.
7. R. A. Soler-Crespo, W. Gao, P. H. Xiao, X. D. Wei, J. T. Paci, G. Henkelman and H. D. Espinosa, *J. Phys. Chem. Lett.*, 2016, **7**, 2702-2707.
8. M. Daly, M. Reeve and C. V. Singh, *Comput. Mater. Sci.*, 2015, **97**, 172-180.
9. T. Zhang and H. J. Gao, *J. Appl. Mech.-T Asme*, 2015, **82**.
10. K. Erickson, R. Erni, Z. Lee, N. Alem, W. Gannett and A. Zettl, *Adv. Mater.*, 2010, **22**, 4467-4472.
11. A. Lerf, H. Y. He, M. Forster and J. Klinowski, *J. Phys. Chem. B*, 1998, **102**, 4477-4482.
12. M. Daly, C. H. Cao, H. Sun, Y. Sun, T. Filleter and C. V. Singh, *ACS Nano*, 2016, **10**, 1939-1947.

13. R. A. Soler-Crespo, W. Gao, L. Mao, H. T. Nguyen, M. R. Roenbeck, J. T. Paci, J. X. Huang, S. T. Nguyen and H. D. Espinosa, *ACS Nano*, 2018, **12**, 6089-6099.
14. C. H. Cao, M. Daly, C. V. Singh, Y. Sun and T. Filleter, *Carbon*, 2015, **81**, 497-504.
15. Z. X. Meng, R. A. Soler-Crespo, W. J. Xia, W. Gao, L. Ruiz, H. D. Espinosa and S. Keten, *Carbon*, 2017, **117**, 476-487.
16. J. T. Paci, T. Belytschko and G. C. Schatz, *J. Phys. Chem. C*, 2007, **111**, 18099-18111.
17. X. D. Wei, L. Mao, R. A. Soler-Crespo, J. T. Paci, J. X. Huang, S. T. Nguyen and H. D. Espinosa, *Nat. Commun.*, 2017, **8**.
18. K. W. Putz, O. C. Compton, M. J. Palmeri, S. T. Nguyen and L. C. Brinson, *Adv. Funct. Mater.*, 2010, **20**, 3322-3329.
19. Y. X. Wang, R. L. Ma, K. S. Hu, S. H. Kim, G. Q. Fang, Z. Z. Shao and V. V. Tsukruk, *ACS Appl. Mater. Inter.*, 2016, **8**, 24962-24973.
20. S. J. Wan, J. S. Peng, Y. C. Li, H. Hu, L. Jiang and Q. F. Cheng, *ACS Nano*, 2015, **9**, 9830-9836.
21. R. A. Soler-Crespo, L. Mao, J. G. Wen, H. Nguyen, X. Zhang, W. X. D., J. X. Huang, S. T. Nguyen and H. D. Espinosa, *Matter*, in press.
22. E. F. Hacopian, Y. C. Yang, B. Ni, Y. L. Li, X. Li, Q. Chen, H. Guo, J. M. Tour, H. J. Gao and J. Lou, *ACS Nano*, 2018, **12**, 7901-7910.
23. S. J. Wan, H. Hu, J. S. Peng, Y. C. Li, Y. Z. Fan, L. Jiang and Q. F. Cheng, *Nanoscale*, 2016, **8**, 5649-5656.
24. Y. H. Wu, R. Cao, G. X. Wu, W. C. Huang, Z. Chen, X. M. Yang and Y. F. Tu, *Composites, Part A*, 2016, **88**, 156-164.
25. A. M. Diez-Pascual and A. L. Diez-Vicente, *ACS Appl. Mater. Inter.*, 2016, **8**, 17902-17914.
26. R. Auhl, R. Everaers, G. S. Grest, K. Kremer and S. J. Plimpton, *J. Chem. Phys.*, 2003, **119**, 12718-12728.
27. V. C. Li, Y. J. Wang and S. Backer, *J. Mech. Phys. Solids*, 1991, **39**, 607-625.
28. M. Rubinstein and R. H. Colby, *Polymer physics*, Oxford University Press, New York, 2003.
29. K. Karatasos and G. Kritikos, *RSC Adv.*, 2016, **6**, 109267-109277.
30. A. Milchev and K. Binder, *Macromolecules*, 1996, **29**, 343-354.
31. J. R. Rice, *J. Appl. Mech.*, 1968, **35**, 379-386.
32. T. L. Anderson, *Fracture mechanics: fundamentals and applications*, CRC press, 2017.
33. G. Bao and Z. Suo, *Appl. Mech. Rev.*, 1992, **45**, 355-366.
34. I. Benedetti, H. Nguyen, R. A. Soler-Crespo, W. Gao, L. Mao, A. Ghasemi, J. Wen, S. Nguyen and H. D. Espinosa, *J. Mech. Phys. Solids*, 2018, **112**, 66-88.
35. D. C. Montgomery, *Design and analysis of experiments*, John Wiley & Sons, 2017.
36. S.-H. Cheng and C. Sun, *J. Nanomech. Micromech.*, 2013, **4**, A4014001.
37. A. Erbas, D. Horinek and R. R. Netz, *J. Am. Chem. Soc.*, 2012, **134**, 623-630.
38. S. Keten and M. J. Buehler, *Nano Lett.*, 2008, **8**, 743-748.
39. We note that while the trends for E/N and F/N data track well with each other, they cannot be directly compared as E/N data were calculated based on only two data points: one at the beginning of the pull-off experiment and the other when the polymer chain was completely off the surface. In contrast, the F/N data was based on a moving average throughout the whole experiment.
40. R. Sinko and S. Keten, *J. Mech. Phys. Solids*, 2015, **78**, 526-539.
41. L. L. Cao, Y. L. Wang, P. Dong, S. Vinod, J. T. Tijerina, P. M. Ajayan, Z. P. Xu and J. Lou, *Small*, 2016, **12**, 3723-3731.
42. P. S. Owuor, C. F. Woellner, T. Li, S. Vinod, S. Ozden, S. Kosolwattana, S. Bhowmick, L. X. Duy, R. V. Salvatierra, B. Q. Wei, S. A. S. Asif, J. M. Tour, R. Vajtai, J. Lou, D. S. Galvao, C. S. Tiwary and P. M. Ajayan, *Adv. Mater. Interfaces*, 2017, **4**, 1700030.
43. O. C. Compton, S. W. Cranford, K. W. Putz, Z. An, L. C. Brinson, M. J. Buehler and S. T. Nguyen, *ACS Nano*, 2012, **6**, 2008-2019.
44. A. Luzar and D. Chandler, *Nature*, 1996, **379**, 55-57.
45. M. L. Zhang, X. T. Wang, C. Y. Li, Y. L. Bai, B. W. Cheng and Z. H. Li, *RSC Adv.*, 2016, **6**, 92378-92386.
46. We note that we intentionally restricted the polymers in our simulations to be 'flexible' so as to maximize the interaction between them and GO. As a result, rigid π-conjugated polymer systems, such as halloysite-polyaniline, which was recently reported to enhance the tensile strength of GO paper by ~2 times (see: C. Wu, T. Zhou, Y. Du, S. Dou, H. Zhang, L. Jiang and Q. Cheng, Nano Energy, 2019, 58, 517-527), was not investigated.
47. K. Vanommeslaeghe, E. Hatcher, C. Acharya, S. Kundu, S. Zhong, J. Shim, E. Darian, O. Guvench, P. Lopes, I. Vorobyov and A. D. MacKerell, *J. Comput. Chem.*, 2010, **31**, 671-690.
48. K. Vanommeslaeghe, E. P. Raman and A. D. MacKerell, *J. Chem. Inf. Model.*, 2012, **52**, 3155-3168.
49. W. Yu, X. He, K. Vanommeslaeghe and A. D. MacKerell Jr, *J. Comput. Chem.*, 2012, **33**, 2451-2468.
50. A. F. Fonseca, T. Liang, D. F. Zhang, K. Choudhary and S. B. Sinnott, *Comput. Mater. Sci.*, 2016, **114**, 236-243.
51. S. Plimpton, *J. Comput. Phys.*, 1995, **117**, 1-19.
52. A. Stukowski, *Modell. Simul. Mater. Sci. Eng.*, 2009, **18**, 015012.

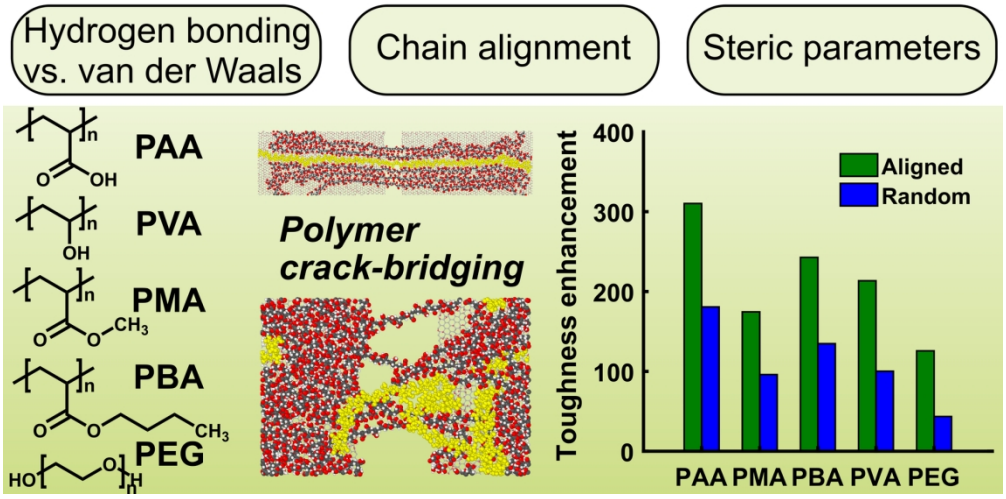

80x40mm (600 x 600 DPI)